

Crystal Orientation and Some Properties of Solid-State Extrudate of Linear Polyethylene

K. IMADA, T. YAMAMOTO, K. SHIGEMATSU, M. TAKAYANAGI
Faculty of Engineering, Kyushu University, Fukuoka, Japan

Transparent and highly oriented samples of high dimensional stability were obtained by extruding crystallised linear polyethylene through a tapered die at temperatures higher than 80°C and below the melting point. The crystal orientation of the extrudate was examined by X-ray techniques, and it was found that there was a preferential *a*-axes orientation parallel to the radial direction of the rod-shaped extrudate. Electron micrographs of the fractured surface of the extrudate revealed closely packed thin fibrils of diameters of about 300 Å. Small angle X-ray scattering showed a long period of 200 to 300 Å along the longitudinal direction of fibrils, depending on the extruding conditions. This fact suggests the existence of the lamellar structure in the fibrils.

1. Introduction

Transparent and well oriented samples were obtained by extruding highly crystallised polyethylene through a tapered die at temperatures higher than 80°C and below the melting point [1]. The purpose of this report is to describe the properties of the extrudate, especially those concerning the crystal orientation, and to discuss the processes through which the crystal orientation was attained.

Studies on the processing of solid state high polymers (cold processing) were carried out in general at room temperature [2]. In these experiments the degree of processing did not exceed the limit which was attainable by stretching. Consequently, the properties of those extrudates were not very different from those of the usual samples obtain by stretching.

Several years ago Takayanagi *et al* studied the conditions of stretching of some crystalline polymers, in connection with the temperature dispersion of the tensile storage modulus at 110 Hz [3]. They concluded that the best condition of stretching, to obtain the highest orientation, modulus value, and ultimate strength, is formed near the temperature at which the crystalline dispersion of the modulus takes place, owing to the change of crystal properties from an elastic state to a viscoelastic one. In experiments on solid state extrusion of crystalline polymers it

will be also important to consider the extrusion temperature. In fact, the importance of the condition of the processing temperature was noticed in our preliminary experiments on solid state extrusion [1]. In those experiments linear polyethylene was found to be successfully extruded to a high degree of processing at temperatures higher than 80°C, while at temperatures lower than 80°C the extrusion failed even for a lower degree of processing. The extrudates thus obtained at approximately high temperatures showed extremely high degrees of orientation and some characteristic features different from those of the usual stretched polymers.

Our experiments on solid state extrusion resemble the extrusion of polyethylene carried out by Porter *et al* [4] with a capillary die at the temperatures close to the melting point, where they are primarily interested in oriented crystallisation. The differences of their experiments from ours are as follows. In our solid state extrusion the material deforms without melting, while in the experiments of Porter [4] the polymer is in a molten state before entering the die, followed by crystallisation under deformation in the die. Experiments of rolling and annealing of linear polyethylene were reported by Keller *et al* [5]. Their work resembles this work in the deformation of solid polymers.

Although the rolling process seems to be largely different from extrusion through a die, there will be an expected common tendency in the orientation process of crystals if the deformation is considered to proceed through slippage along special lattice planes in both cases.

From these points of view we will discuss the crystal orientation of solid state extrusion of linear polyethylene.

2. Experimental

2.1. Materials

High density polyethylene, Hizex 1200J (Mitsui Petrochemical Co, Ltd), was used as the material to be extruded. The samples of melt indices (MI) 4 and 0.4 of another high density polyethylene, Novatec (Mitsubishi Kasei Co, Ltd), were also used in some preliminary experiments. The degree of branching of these polymers was as low as 2 CH₃ per 1000 CH₂.

Billets of the polymer were cut out from the moulded rod. The diameter of the billets was 9.9 mm and the lengths ranged from 20 to 30 mm. The density of these billets evaluated by the floating method was 0.96 g/cm³ and their crystallinity was estimated to be 71%.

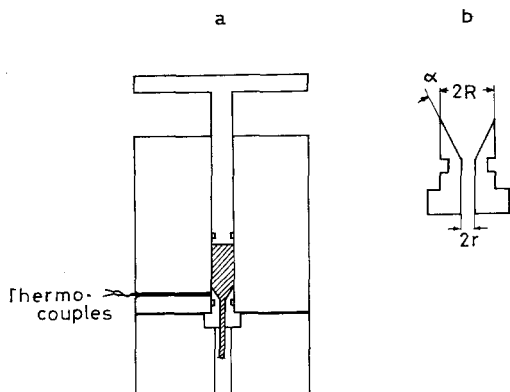


Figure 1 Device used for extrusion experiments (a) piston, cylinder, and die assembly (b) vertical section of die.

2.2. Extruding Device and Extrusion Experiments

Fig. 1 shows the device used for the extrusion experiments. The inner diameter of the cylinder was $2R = 10$ mm, and the outer diameter was 80 mm. The cylinder was charged with the billet and heated with a ribbon heater wound around the cylinder. The piston was pressed into the cylinder by placing the device between the plates

of the oil press. The plates were heated with electrical heaters installed in them and kept at the extrusion temperature.

The temperature of the die piece was measured with a Copper-Constantan thermocouple inserted into the hole drilled into the cylinder wall, with the probe touching the outer wall of the die. The extrusion temperature was controlled with an accuracy of $\pm 1^\circ\text{C}$. The length of the extrudate was measured from the outlet of the die to the top of the extruded sample.

Fig. 1b shows a section of the die piece. The diameter of the entrance was about 9 mm and that of the exit was $2r = 2.0, 2.5, 3.0, 4.0,$ or 4.5 mm. The entrance angle of die α was always 20° .

Silicon vacuum grease, of Dow Corning Co, was used as a lubricant. Both the die hole and the billet were smeared with the grease before they were set up for the experiments.

2.3. Definition of the Degree of Processing

It will be convenient to define the value which expresses the degree of processing in order to compare it with the draw ratio of the stretched samples. In the case of the extrusion the ratio of the cross sectional area before and after the processing is defined as the degree of processing. This will be expressed as $(\pi R^2)/(\pi r^2) = (R/r)^2$, where R and r are the radii of the sample before and after extrusion, respectively.

The degree of the deformation of the sample is also expressed in terms of the so-called true strain, or logarithmic strain as follows:

$$\epsilon = \int_{l_0}^l \frac{dl}{l} = -2 \int_R^r \frac{dr}{r} = 2 \ln (R/r)$$

2.4. Measurements of the Properties of the Extrudate

A specimen holder for fibre samples was used to determine the X-ray diffraction intensity distribution as a function of the sample orientation. The orientation function with respect to the direction of the extrusion was determined for the sample, which was cut out from the extrudate in its central part. The intensity measurement was carried out by rotating the sample around the axis perpendicular to the central axis of the extrudate. Another sample was cut from the outer side of the extrudate for the determination of the crystal orientation with respect to the radial direction of the extrudate. In this case the distribution of the diffraction intensity was

measured by rotating the sample around the axis parallel to the central line of the original extrudate. Although the perfect expression of the intensity distribution over the whole region of the stereographic sphere was not intended here, a simple schematical expression was used for illustrating the three dimensional scheme of the crystal orientation. The outstanding convergence of the *c*-axis orientation to the extrusion direction made it unnecessary to prepare the complete pole figure, which is required in interpreting more complex orientations.

X-ray small angle diffraction was measured with a line slit system (Rigaku Denki Co, Ltd). The sample chips cut from the extrudate were set so that the extrusion direction was perpendicular to the slit, and the GM counter with a receiving slit was scanned in a plane parallel to the extrusion direction.

The structure of the fractured surface of the extrudate was observed under the electron microscope by the method of two step replication using an acetylcellulose film.

For both purposes of viscoelastic and thermal shrinkage measurements the Vibron DDV II was used, with samples of dimensions $0.2 \times 2.0 \times 30$ mm, the long edge of the sample being cut parallel to the extrusion or stretching direction. The rate of the temperature rise during the measurements was $1.5^\circ\text{C}/\text{min}$. The measure-

ments of the thermal shrinkage along the extruded or stretched directions were conducted at the approximately constant tension of less than 10^6 dyne/cm². The tensile storage modulus and the loss modulus were measured at 110 Hz, with the amplitude of about $2 \mu\text{m}$ over a temperature range from -170 to 130°C . The mechanical relaxation curves were used to check the difference between the structures of the solid-state extrudate and the drawn sample.

DTA measurements were carried out with an instrument constructed by Takamizawa which required very small samples, e.g. 1 mg. Comparisons of the melting temperatures and heats of fusion of the samples taken from various parts of the billet were made from measurements of the position of the peak height and the area under the exothermic curve respectively.

Densities were measured by the floating method at 25°C in a mixture of water and ethanol.

3. Results and Discussion

3.1. Crystal Orientation

Fig. 2 shows the process of the development of the crystal orientation in the die hole. The sample was Novatec (MI = 4), and the extrusion was conducted at 80°C . The X-ray diffraction patterns are placed at their corresponding location on a profile of the longitudinal section of the extrudate. The test pieces for the X-ray diffraction were cut out from the polymer cone, which was taken out of the die hole after interrupting the extrusion. As shown in the diagram the degrees of the *c*-axis orientation are almost the same at the centre and the wall side.

Table I gives the values of the orientation functions of the extrudates obtained at different extruding conditions and those of the hot drawn sample, which was prepared by drawing the bulk sample at 80°C by a factor of 10. The symbols of f_c , f_a , and f_b in the table denote the orientation functions of the axes *c*, *a*, and *b* with respect to the extrusion direction. In the special case of perfect orientation of the *c*-axis, and random orientation of *a*- and *b*-axes around the *c*-axis, the functions take the values of $f_c = 1$, and $f_a = f_b = -0.5$. According to Table I, the extrudates display a very high degree of *c*-axis orientation and especially that extruded at 110°C with the degree of processing 16 shows the highest *c*-axis orientation.

Next, the axial symmetry of the orientation of the crystal planes will be discussed. Fig. 3 shows

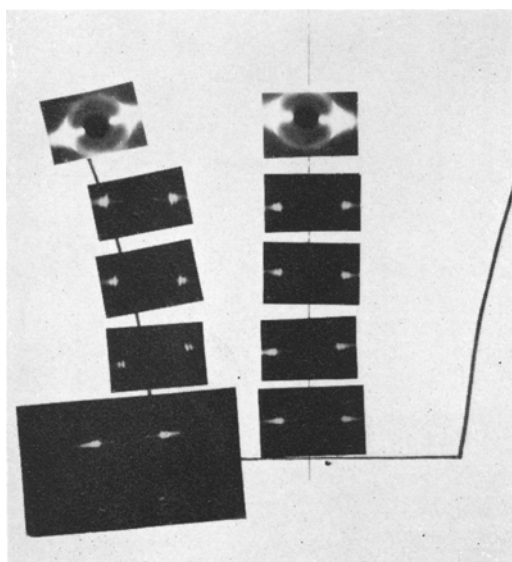


Figure 2 Diagram showing development of *c*-axis orientation during the progress of extrusion.

TABLE I Orientation functions of extruded and drawn samples

(a) Extruded samples				
Extruding temp, °C	Degree of processing, $\left(\frac{R}{r}\right)^2$	f_c	f_a	f_b
110	16	0.990	-0.495	-0.495
100	16	0.970	-0.495	-0.485
80	16	0.994	-0.496	-0.497
100	6.25	0.960	-0.485	-0.476
80	6.25	0.938	-0.485	-0.454

(b) Drawn sample				
Drawing temp, °C	Draw ratio α	f_c	f_a	f_b
80	10	0.985	-0.496	-0.489

R = 10 mm

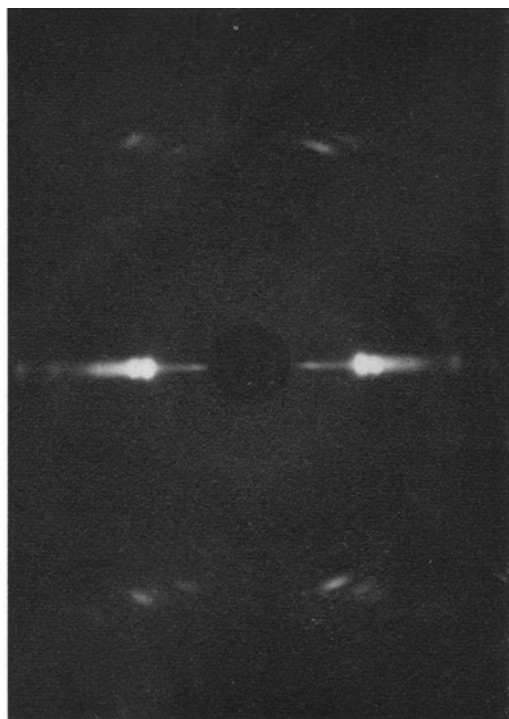
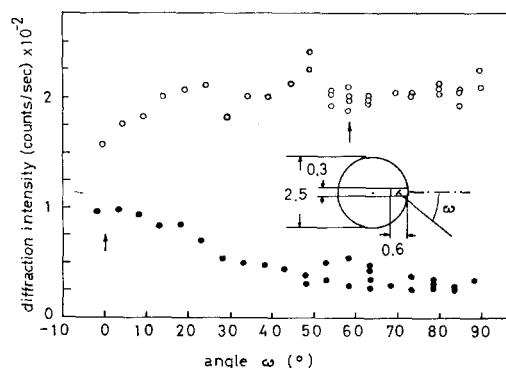


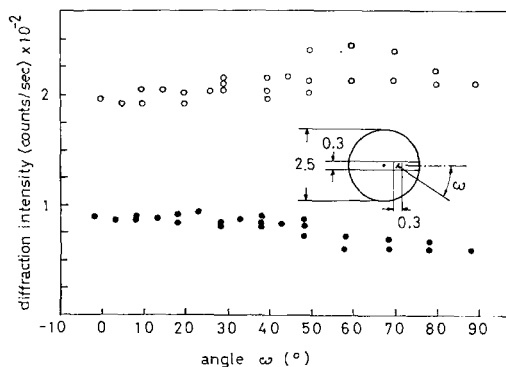
Figure 3 X-ray diffraction pattern of the specimen taken from the outer region of the extrudate.

the fibre diagram which is the enlarged one of the photograph cited at the lowest position on the wall side in fig. 2. In the diagram of fig. 3, it is noticed that the intensities of the layer line reflections are not symmetrical. The intensities of the reflections of (011), (111), and (121) planes are stronger on the right side than the left side,

while those of the (201) reflection is in a reversed relation, being stronger on the left side than the right side. The equatorial reflections such as (020) show the same intensity relation as the (011). This fact suggests the presence of some preferential orientation of the crystal planes. To study this phenomenon in more detail, a thin specimen was cut out from the wall wide region of the extrudate, and the distribution of the diffraction intensities around the axis parallel to the extrusion direction were observed.



(a)



(b)

Figure 4 Distribution of X-ray diffraction intensity as a function of angle ω between the plane normal and radial direction of the specimen taken from (a) outermost region and (b) inside region of the extrudate. \circ , 110; \bullet , 200.

Fig. 4a shows the intensity distribution of the (200) plane (filled circles) and the (110) plane (open circles). The test piece used is 0.6 mm thick in a radial direction, being cut out from the outermost region of the rod of 2.5 mm diameter. The angle of the abscissa is taken as the angle between the plane normal and the radial direction. When $\omega = 0$, the plane in question is perpen-

pendicular to the radial direction. From fig. 4, it is revealed that the a -axis is preferentially oriented along the radial direction, as the intensities of (200) planes show a maximum around $\omega = 0$. If we assume that a simple preferential orientation of (200) plane, the intensity of (110) planes should have the maximum at around $\omega = 56^\circ$ (as indicated by the arrow in the figure). Actually the reflections of the (110) plane show the tendency to increase in intensity with increasing angle ω according to simple geometrical relations. It should be noticed, however, that the intensities of the (110) planes have no sharp maximum, but rather increase towards larger and smaller angles from $\omega = 56^\circ$, showing a broad maximum at about 23° and 80° . This fact seems to suggest a more complex orientation. Fig. 5 shows the schematical pole figures of the {200} and {110} planes, which are prepared to satisfy the intensity relation of fig. 4a and by taking account of the values of the f_a and f_b being almost -0.5 , and that of the f_c being almost 1.0 . Although the fact of the coexistence of the crystals with different orientations is not yet

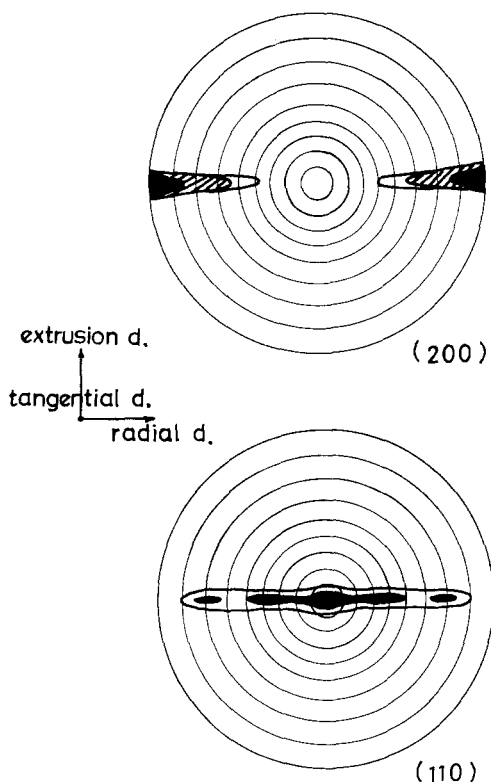


Figure 5 Schematical representation of intensity distribution of (a) 110 and (b) 200 diffraction on the stereographic nets.

clarified, some specified lattice planes other than the {200} plane, such as {310} or {210} planes, are considered to participate in the deformation process as the sliding planes. If the assumption of the multiple orientation of the {310} plane besides {200} is true, the distribution of the normals of the {110} planes will take the maximum at $\omega = 29.5^\circ$ and 82.0° and that of the {200} plane at $\omega = 26.0^\circ$. The latter expected maximum does not appear as an isolated peak, but its contribution can be seen in that the intensity distributions of the {110} plane normal only starts decreasing below 25° .

The process of twinning, as suggested by Keller *et al* [5] for cold-rolled samples could not be found. However, in our case, there is an annealing effect in addition to the deformation process within the die.

The results shown in fig. 4b are on the specimen 0.3 mm thick cut out from the inner part of the extrudate, at the place 0.6 mm apart from the wall side surface. As a matter of course the axial distributions of the orientation of the {110} and {200} planes become much more difficult to observe, when the sample chips were taken out from the region near symmetry axis. In spite of this disadvantage the intensity relations of the similar tendency as in fig. 4a is observed also in fig. 4b. Thus the preferential orientation of the crystal planes is not limited in the surface layer, and the most of the crystals are oriented so that the a -axis is parallel to the radial direction. This fact is most characteristic of the solid-state extrudate.

In the process of steady state extrusion through a tapered die, polymer is pressed towards the central axis by the reacting forces from the die wall. Thus the case will be an axially symmetric version of the cases of rolling, or plane compression of the sheets.

As reported by Keller *et al* [5], rolled and annealed samples show remarkable tendency for orientation of the a -axis in the direction of compression between rollers. And the a -axis orientation was also easily observable when we compressed a sample chip at room temperatures between a vice and examine it under compression. In these three cases, i.e. the rolling, the plane compression and the extrusion through the tapered die, there is a common tendency for the orientation of the a -axis to be in the direction of compression. This will suggest that the deformation proceeds in all these cases through the slippage occurring in the crystals along the plane

perpendicular to the a -axis. Such a slipping motion of the specified crystal plane will stop when its direction becomes completely perpendicular to the direction of compression. Thus a -axis orientation will be completed when these conditions are satisfied.

3.2. The Super-Structure of the Extrudate

3.2.1. Transparent Appearance of the Extrudate

The extrudate extruded at the temperatures higher than 80°C and to a degree of processing of 16 showed a transparent appearance for low extrusion rates. Above 90°C higher extrusion rates would also give a transparent extrudate. By inspecting the material taken out from the die hole after interrupting the extrusion, it was obvious that the transparency appears when the degree of processing reached to 14 or 15. Transparency of the extrudate suggests that the extrudate is absent in voids and is composed of the densely packed structural units, which are smaller in dimensions than the wave length of visible light.

3.2.2. Electron Microscopy on the Fractured Surface of the Extrudate

Fig. 6 shows a replica of the fractured surface of the extrudate extruded at 80°C to the degree of processing 16. Fig. 7 shows another example of the replica of the fractured surface of the extrudate, which was, in this case, compressed along the extrusion direction, then fractured. In fig. 7a, kink band is observed running down from left to right. Fig. 8 is an enlargement of part of

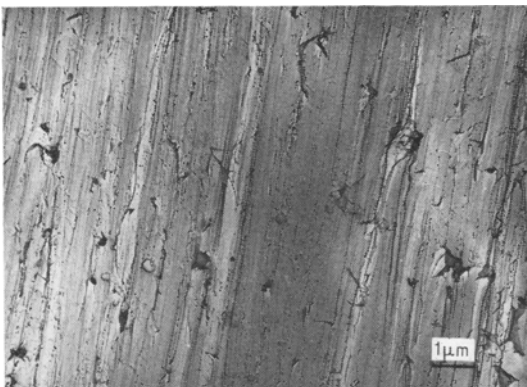


Figure 6 Electronmicrograph of replica of fractured surface of the extrudate. A rod shaped extrudate was fractured along the plane parallel to the direction of extrusion.

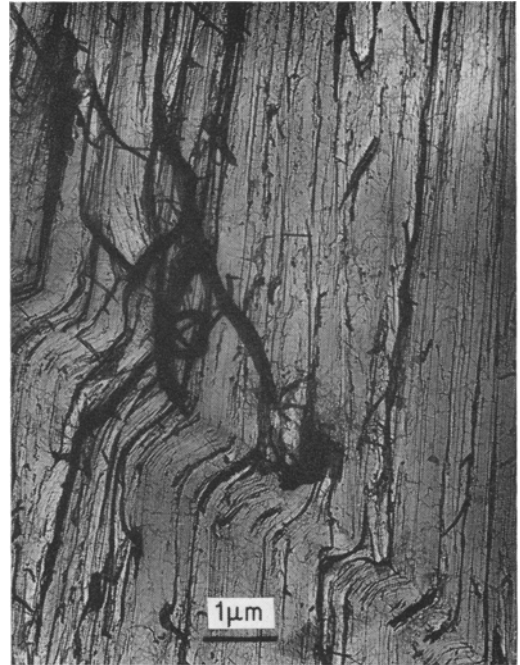


Figure 7 Electronmicrograph of replica of fractured surface of the extrudate, which had been compressed along the extrusion direction to produce "kink band".

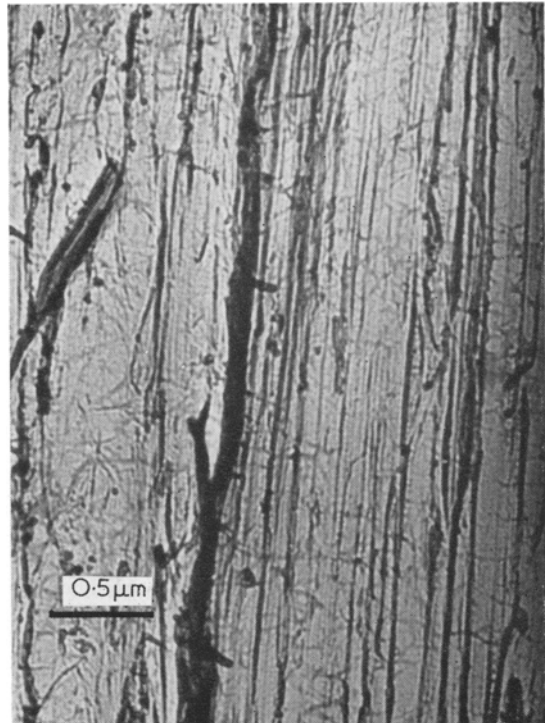


Figure 8 Photograph enlarged from fig. 7.

fig. 7 (upper right). Densely packed microfibrils or striations are observed in several places. Especially, in the enlarged image of fig. 8, microfibrils are clearly discriminated. The diameters of the micro fibres seem to be uniform and are estimated at about 300 Å. Occasionally, fibrous materials remained on the final replicating films. The striations could also be distinguished on it. The electron diffraction pattern of restricted field was obtained on the fibrils with a direct image method, which was the typical fibre pattern. By compressing the extrudate along the extrusion direction the kink band was generated, as shown in fig. 7, such a kink band is in general observable for the highly oriented samples deformed along the fibre axis.

The electromicroscopic observation of the fractured surface gives us the straightforward explanation of the transparent appearance and the highest orientation of the extrudate.

3.2.3. X-Ray Small Angle Scattering

A peak was found in the X-ray diffraction intensity curve obtained by a 2θ scan along the direction of the extrusion, showing a long period

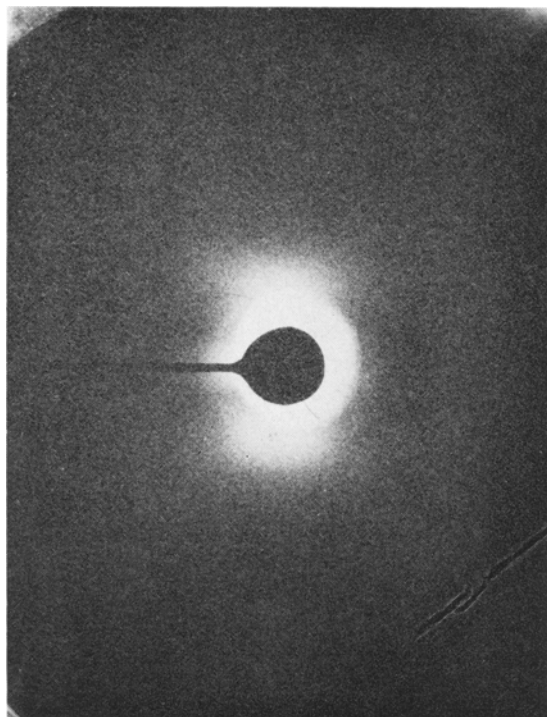


Figure 9 X-ray small angle scattering of the extrudate. Extrusion direction is from the top downward.

of 200 to 300 Å. After the annealing at 120°C a solid extrudate prepared with degree of processing 16 at 100°C was found to have increased in long spacing from 204 to 330 Å. The long period of the drawn sample annealed at 120°C was 290 Å. As in the cases of stretching, the long period increased with increasing extrusion temperature. As far as the long period is concerned there was no remarkable difference between the extrudate and the drawn samples.

Fig. 9 shows the photographic image of X-ray small angle scattering of the extrudate. Meridional diffraction which was elongated horizontally suggests the fluctuations of the special arrangement of tiny lamellar crystal. On the equator the scattering intensity spread horizontally, corresponding to the lateral structure of the densely packed microfibrils.

3.3. Some Properties Concerning the Crystal Orientation and Super-Structure

3.3.1. Density

Table II gives the values of the densities of the extrudates obtained at different conditions. As the lattice dimensions of the crystals in the extrudates were not different from those of the usual melt crystallised samples, the increase in the density of the extrudates is understood as being due to the increase of the crystallinity. The values given in the last column of table II were obtained by assuming the amorphous density $d_a = 0.8565$ g/cc, and the crystal density $d_c = 1.009$ g/cc.

3.3.2. Crystal Melting

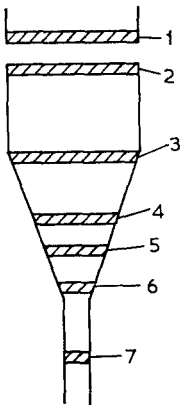
Table III gives a comparison of the melting temperatures and the relative values of heat of fusion among the specimens taken out from the sample, which had been used in an extrusion of the degree of processing 16 carried out at 100°C, at the various locations. It is clear from table III that the perfection of the lamellar crystals

TABLE II Density of Extrudate

Degree of processing, $\left(\frac{R}{r}\right)^2$	Extrusion temp, °C	Density, g/cm ³	Crystallinity, %
16	100	0.973	79.2
16	90	0.966	75.0
16	80	0.969	76.8
6.25	100	0.956	70.7
6.25	80	0.960	71.3

R = 10 mm

TABLE III Melting temperature and heat of fusion of samples at different places in the die

	Sample location	Melting* temp, °C	Heat of fusion† (arbitrary unit)
	1	127.2	0.1793
	2	127.6	0.1894
	3	129.0	0.1840
	4	129.3	0.1832
	5	131.3	0.1936
	6	132.5	0.2146
	7	133.5	0.2040

*Peak temperature of DTA thermogram

†The area of the fusion peak in the DTA thermogram, compared on the basis of the unit weight of the samples.

increases with the increase of the degree of orientation, as it was observed in the increase of the melting temperatures, together with the progress of the extrusion. The melting temperature takes the maximum value at the die exit.

The extrudates of the higher degrees of processing, and those obtained at the higher extrusion temperatures showed higher melting temperatures and the larger heat of fusion. These effects are explained as the extrusion conducted at the increased temperatures and pressures give the superstructures in which the crystals were larger and more perfect than the extrudates obtained at lower temperatures and pressures.

3.3.3. Thermal Shrinkage

An extraordinary feature of the extrudate is its high dimensional stability. In fig. 10 the thermal shrinkage is shown as a function of the temperature for the sample extruded at 110°C with the degree of processing 16 (filled circles). The shrinkage of the drawn sample which was obtained by stretching the sample to ten times its original length is also shown for comparison (open circles). The stretched sample began to shrink at about 60°C, which is below the temperature at which the specimen had been stretched, while the sample extruded at 110°C did not shrink, even at the temperatures as high as 110°C, it finally began to shrink at about 120°C. This temperature agrees with the temperature where the DTA thermogram devi-

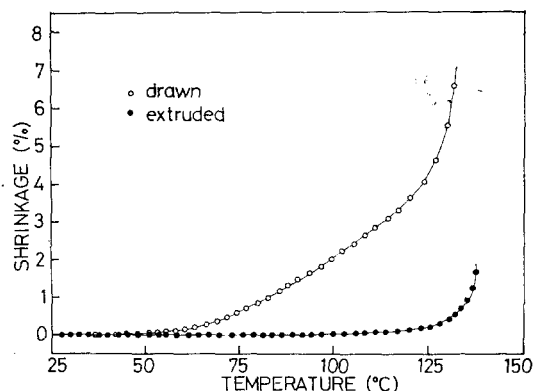


Figure 10 Shrinkage of the extruded and the drawn samples during the temperature rise of the rate of 1.5°C/min. ○, drawn; ●, extruded. Drawing temperature was 80°C, and extrusion temperature 100°C. Drawing ratio was 10 and the degree of processing 16.

ates from the background towards the endothermic peak. This temperature region also corresponds to that where the long period of the extrusion direction begins to increase. Thus the phenomenon of the shrinkage of the extrudate is considered to be associated with the thermal motion of the molecules in the crystals. On the other hand, the remarkable shrinkage of drawn samples, which was observed at the temperatures as low as 60°C, will be due to the relaxation of the strained molecular chains in the amorphous phase.

From these comparisons of the shrinkage behaviour, the super-structure of a microfibril in the extrudate is assumed to be constructed from the well developed, and highly oriented, lamellar crystals with a small amount of the relaxed amorphous phases filling the spaces among them.

3.3.4. Tensile Modulus of the Extrudate

As the crystals in the extrudate become highly oriented in the direction of the extrusion, the modulus of the extrudate along this direction is expected to be very high. Fig. 11 shows the comparison of the stress-strain relations of the extrudate, the unoriented original sample, and the cold drawn sample. The tensile modulus of the extrudate at the stretching velocity of 5 mm/min and at room temperature is about 3×10^{11} dyne/cm².

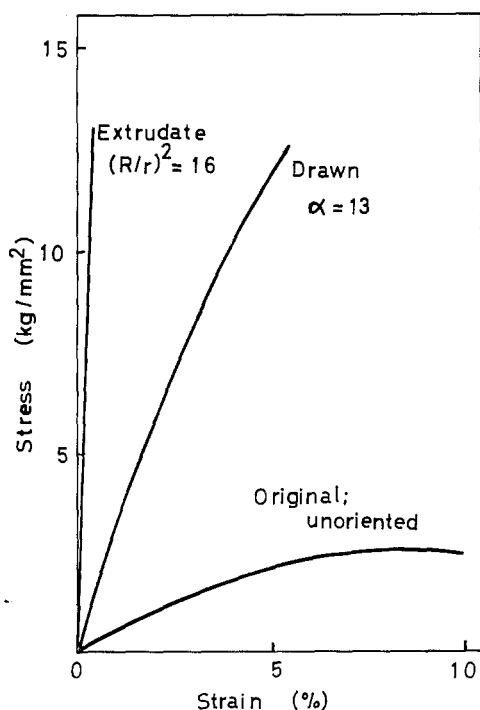


Figure 11 Stress-strain curve of original (undrawn), cold-drawn, and extruded samples. Extruding temperature was 100°C and the degree of processing 16.

The tensile storage modulus at 110 Hz and at room temperature is also in the order of the magnitude of 10^{11} dyne/cm². The loss modulus shows a crystalline absorption at about 100°C

and a low temperature secondary absorption at about -130°C. It was found unexpectedly that there was no remarkable differences between extrudates and well annealed highly oriented samples.

4. Summary and Conclusions

- (1) Extrudates obtained by extruding linear polyethylene in a solid state at temperatures higher than 90°C and below the melting point with the degree of processing as high as 16 showed the highest degree of crystal orientation (*c*-axis) and an outstanding dimensional stability.
 - (2) The extrudate showed the tendency of preferential orientation of the planes such as {200}, and {310} or {210}, suggesting a possible mechanism of plastic deformation along these planes to align normal to the radial direction.
 - (3) Microfibrils with comparatively uniform diameters of about 300 Å were observed with the electron microscope both on the replica of the fractured surface and the fibrous materials remained on the replica.
 - (4) Long periods of 200 to 300 Å was observed along the longitudinal direction of the microfibrils, showing the existence of the crystal lamellae of this thickness and of small diameter. Increase in the long period by annealing was observed above 120°C. The samples annealed at 120°C showed the long period of 300 Å.
 - (5) Highest dimensional stability of the extrudate up to 120°C may be due to the annealing effect of stabilising the super-structure during the extrusion process in the die hole.
 - (6) To clarify the mechanisms of the plastic deformation of the polymeric materials with high crystallinity, it is necessary to analyse the characteristics of the extrusion processes, in addition to the effort to reveal the detailed crystal orientation scheme.
- Analysis of the extrusion process will be reported in another paper in preparation.

Acknowledgement

The authors wish to thank Professor T. Oyama and Professor K. Takamizawa for their kindness in offering the DTA instrument constructed by them. The authors are also indebted to D. Matsukuma, K. Ueno, and K. Kanekiyo in our laboratory, and S. Nakamura for their help in conducting the extrusion experiments and making the devices. The fund of this work was supported by the Association of Asahi Glass for the Advancement of Engineering, the Mitsubishi

Chemical Industries Limited, and the Ministry of Education, Japan.

References

1. K. IMADA, M. TAKAYANAGI, and T. YAMAMOTO, a paper presented at the 18th Annual Meeting of the Society of Polymer Science, Japan (May 1969, Tokyo).
K. IMADA, T. YAMAMOTO, K. UENO, D. MATSUKUMA, and M. TAKAYANAGI, *J. Soc. Mater. Sci. Japan* **19** (1970) 302.
Idem, *Rep. Prog. Polymer Phys. Japan* in press (1970).
2. A. BUCKLEY and H. A. LONG, *Polymer Eng. Sci.* **9** (1969) 115.
V. E. MALPASS, *Appl. Polymer Symposia* **12** (1969) 19.
T. MAEDA, *Plastics Age (Japan)* **15** No. 11 (1969) p. 55.
3. M. TAKAYANAGI, S. MINAMI, and F. NAGATOSHI, *Reports of the Association of Asahi Glass Company for the Advancement of Engineering Japan* **7** (1961) 127.
M. TAKAYANAGI, S. MINAMI, and K. KUGA, *ibid* **8** (1962) 97.
4. J. SOUTHERN and R. S. PORTER, *ACS Polymer Preprints* **10** No. 2 (1969) 1028.
5. J. J. POINT, D. GEZOVICH, A. KELLER, and G. A. HOMES, *J. Mater. Sci.* **4** (1969) 908.
I. L. HAY and A. KELLER, *J. Mater. Sci.* **1** (1966) 41.

Received 23 November 1970 and accepted 15 March 1971.